Resonances in the Λnn system

Iraj R. Afnan and Benjamin F. Gibson

Resonances in the Λnn system

Iraj R. Afnan[*]

School of Chemical and Physical Sciences,

Flinders University, GPO Box 2100, Adelaide 5001, Australia

Benjamin F. Gibson[†]

Theoretical Division, Los Alamos National Laboratory,

Los Alamos, NM 87545, USA

Abstract

Background: A bound state of the Λnn system has been reported, but at least three theoretical papers question the existence of such a bound state.

Purpose: We address the alternative question of whether there might exist a resonance in the Λnn system, using a rank one separable potential formulation of the Hamiltonian.

Methods: We examine the eigenvalues of the kernel of the Faddeev equation in the complex energy plane using contour rotation to allow us to analytically continue the kernel onto the second energy sheet. The model Λn interaction is fitted to the Λp scattering length and effective range.

Results: We follow the largest eigenvalue as the Λn potentials are scaled and the Λnn continuum is turned first into a resonance, and then into a bound state of the system.

Conclusions: Because a change in the strength of the Λn potential of as little as 5% will produce a Λnn resonance, we infer that an experiment of the ^{3}H(e,e'K$^+$)$_\Lambda^3$n type at JLAB could be used to constrain the properties of the Λn interaction.

[*] Iraj.Afnan@Flinders.edu.au

[†] bfgibson@lanl.gov

I. INTRODUCTION

A recent experiment has suggested that there is a bound state of the Λnn system [1], whereas several theoretical analyses demonstrate that such a bound state cannot exist [2–4]. Because the hypertriton is a just bound $T = 0$ state $[B_\Lambda(^3_\Lambda H) = 0.13 \pm 0.05$ MeV], we do not expect the $T = 1$ Λnn system to be bound, because in going from the $T = 0$ state to the $T = 1$ state we must replace the $^3S_1$-$^3D_1$ np interaction, which supports a bound state, by the $^1S_0$ nn interaction that has an anti-bound state. The question we would like to address is: Could there be a three-body resonance in the $T = 1$ Λnn system even though all the interactions are predominantly s-wave? To examine this possibility, we consider the Λnn system with the pairwise interactions being rank one separable potentials that fit effective range parameters of the nn system and those predicted by different Nijmegen one-boson exchange potentials for the Λn system [5, 6], or the Jülich one-boson exchange potential [7] and chiral ΛN potential [8]. The use of rank one separable potentials allows us to very simply analytically continue the Faddeev equations into the second complex energy plane in search of resonance poles by examining the eigenvalue spectrum of the kernel of the Faddeev equations, as we did previously for Λd scattering [9].

II. RANK ONE SEPARABLE POTENTIALS

Because we will use rank one separable potentials in this study, we review briefly the rank one Yamaguchi potential [10] that will be used to fit the scattering length and effective range of the nn and Λn interactions. This rank one S-wave potential has the form

$$V(k, k') = g(k)\, C\, g(k') \quad \text{with} \quad g(k) = \frac{1}{k^2 + \beta^2} \,, \tag{1}$$

where C is the strength of the potential and β is the 'range' of the potential. The on-shell t matrix $T(k_0)$ for this potential is given by

$$T(k_0) = g(k_0)\, \tau(E^+)\, g(k_0) \,, \tag{2}$$

where the on-shell momentum k_0 is defined in terms of the energy $E = \frac{k_0^2}{2\mu}$, with μ being the reduced mass. The function $\tau(E^+)$ is given by

$$\tau(E^+) = \left\{ C^{-1} - 2\mu \int_0^\infty dk\, k^2\, \frac{[g(k)]^2}{k_0^2 + i\epsilon - k^2} \right\}^{-1} . \tag{3}$$

For the form factor $g(k)$ defined in Eq. (1), the integral in Eq. (3) becomes

$$2\mu \int_0^\infty dk\, k^2 \frac{[g(k)]^2}{k_0^2 + i\epsilon - k^2} = \frac{\pi\mu}{(k_0^2 + \beta^2)^2} \left(\frac{k_0^2 - \beta^2}{2\beta} - i\,k_0 \right) . \tag{4}$$

This allows us to write the on-shell t matrix as

$$T(k_0) = \left\{ C^{-1} \left(k_0^2 + \beta^2 \right) - \pi\mu \left(\frac{k_0^2 - \beta^2}{2\beta} - i\,k_0 \right) \right\}^{-1} . \tag{5}$$

Making use of the fact that the S-wave scattering amplitude can be written in terms of the phase shifts as

$$f_0(k_0) = e^{i\delta_0} \sin \delta_0 = \frac{1}{\cot \delta_0 - i} = -\pi\mu\, k_0\, T(k_0) , \tag{6}$$

we can express $k_0 \cot \delta_0$ as

$$k_0 \cot \delta_0 = -\frac{\beta}{2} \left(1 + \frac{2\beta^3}{\pi\mu\, C} \right) + \frac{1}{2\beta} \left(1 - \frac{4\beta^3}{\pi\mu\, C} \right) k_0^2 - \frac{k_0^4}{\pi\mu\, C} \tag{7}$$

$$\approx -\frac{1}{a} + \frac{1}{2}\, r\, k_0^2 . \tag{8}$$

We now can extract by inspection the scattering length a and the effective range r for the Yamaguchi potential obtaining

$$\frac{1}{a} = \frac{\beta}{2} \left(1 + \frac{2\beta^3}{\pi\mu\, C} \right) \quad \text{and} \quad r = \frac{1}{\beta} \left(1 - \frac{4\beta^3}{\pi\mu\, C} \right) . \tag{9}$$

We can eliminate the strength of the potential and get a quadratics in β with a solution

$$\beta = \frac{1}{2r} \left[3 \pm \sqrt{9 - 16\frac{r}{a}} \right] . \tag{10}$$

Because a can be negative, we must take the $+$ sign to get a positive β. Therefore, we have

$$\beta = \frac{1}{2r} \left[3 + \sqrt{9 - 16\frac{r}{a}} \right] . \tag{11}$$

We now can solve for the strength of the Yamaguchi potential to obtain

$$C = \frac{4\,\beta^3}{\pi\mu\,(1 - \beta\,r)} . \tag{12}$$

For the $^1S_0$ np system with scattering length $a_s = -23.715$ fm and effective range $r_s = 2.73$ fm, the parameters of the Yamaguchi potential are

$$\beta_{np} = 1.1525 \text{ fm}^{-1} \quad \text{and} \quad C_{np} = -0.3817 \text{ fm}^{-2} . \tag{13}$$

3

On the other hand, for the nn system we have a singlet scattering length and effective range [12] of $a_s = -18.9 \pm 0.4$ fm and $r_s = 2.75 \pm 0.11$ fm, which results in Yamaguchi potential parameters given by

$$\beta_{nn} = 1.1574 \text{ fm} \quad \text{and} \quad C_{nn} = -0.37986 \text{ fm}^{-2} . \tag{14}$$

The effective range parameters for the Nijmegen Model D hyperon-nucleon potential [5] suggest that there is some charge symmetry breaking in the data. Therefore, we consider rank one Yamaguchi potential fits to the singlet and triplet effective range parameters for both the Λn and Λp systems. In Table I we provide the effective range parameters as reported by the Nijmegen group [5] and the parameters of the corresponding Yamaguchi [10] potentials. Note that the poles of the amplitude are on the negative imaginary axis; *i.e.*, there are no bound states in the Λn and Λp systems.

TABLE I. The effective range parameters for the Λn and Λp systems as given by the Nijmegen model D potential [5]. Also included in the table are the parameters of the Yamaguchi potential determined from the effective range parameters. In addition we report the closest pole to the real axis as extracted from the full amplitude $T(k_0)$.

	Λp	Λn
a_s	-1.77 ± 0.28	-2.03 ± 0.32
r_s	3.78 ± 0.35	3.66 ± 0.32
Pole	$-0.3439\,i$	$-0.3155\,i$
β_s fm^{-1}	1.2659	1.2503
C_s fm^{-2}	-0.2642	-0.2692
a_t	-2.06 ± 0.12	-1.84 ± 0.10
r_t	3.18 ± 0.12	3.32 ± 0.11
Pole	$-0.3231\,i$	$-0.3479\,i$
β_t fm^{-1}	1.3844	1.3786
C_t fm^{-2}	-0.3844	-0.3608

III.   THE HYPERTRITON

Before proceeding with our investigation of the Λnn system, we compare the results of our code with those of our previous examination of the hypertriton [11]. Here we consider only the Λnp system with no $\Lambda N - \Sigma N$ coupling. We make use of the NN and ΛN potentials defined in Tables IV and VI of Ref.[11]. For the case when both the np and ΛN potential have a tensor force (*i.e.*, $^3S_1$ - $^3D_1$) we obtain a binding energy of 2.326 MeV to be compared with 2.329 MeV of Ref.[11].

Next, we establish the fact that using a separable potential yielding the effective range parameters for the NN and ΛN interaction is not a drastic approximation. Here we use the recent tabulation of the effective range parameters of the chiral models for the ΛN interaction and the corresponding hypertriton binding energies in Table 6 of Ref.[8]. The agreement (See Table II) between the result using the Yamaguchi potential and the more exact calculation for the binding energy of $^3_\Lambda$H is reasonable considering that the calculations are based on the Yamaguchi potential with and without the tensor coupling in the NN interaction. As anticipated, the inclusion of the tensor force in the $^3S_1$-$^3D_1$ NN interaction improves the agreement with the more exact calculation. Note that we have not included any $\Lambda N - \Sigma N$ coupling or any three-body forces in the calculation.

Having established the validity of using a Yamaguchi type potential to calculate the hypertriton binding energy, we turn in the next section to investigate the possible existence of a resonance in the $T = 1$ channel, (*i.e.*, the Λnn system). The advantage of using a Yamaguchi type potential is that we can analytically continue the Faddeev equations onto the second sheet of the complex energy plane with minimal effort.

IV.   POTENTIAL RESONANCES IN THE Λnn SYSTEM

To investigate the possibility of a Λnn resonance, we must analytically continue the Faddeev equations for this system onto the second energy sheet, and examine the eigenvalue of the kernel on this exposed second Riemann sheet [13]. For Yamaguchi type pairwise interactions with two identical Fermions, the homogenous Faddeev integral equations take

TABLE II. Comparison of the binding energy of the hypertriton using a chiral interaction or boson-exchange interaction with results for separable potentials that yield the same effective range parameters. The final three lines are the results for Yamaguchi NN with 7%, 4% and 0% D-state probability for the deuteron. The ΛN potentials are those that fit the effective range parameters in the table with no tensor force. Also included in the table are the Yamaguchi parameters for the ΛN potentials used to calculate the binding energy of $^3_\Lambda$H.

ΛN Potential	Chiral($\Lambda = 600$)	Nijmegen Model D	Jülich04	Nijmegen NSC97f
a_s	-2.91	-2.03	-2.56	-2.60
r_s	2.78	3.66	2.74	3.05
β_s	1.4259	1.2503	1.4802	1.3557
C_s	-0.4818	-0.2692	-0.5228	-0.3915
a_t	-1.54	-1.84	-1.67	-1.72
r_t	2.72	3.32	2.93	3.32
β_t	1.6735	1.3786	1.5510	1.4029
C_t	-0.6500	-0.3608	-0.5186	-0.3719
B.E.($^3_\Lambda$H)	2.30	–	2.27	2.30
B.E.(YY $P_D = 7\%$)	2.77	2.31	2.65	2.55
B.E. (YY $P_D = 4\%$)	2.88	2.33	2.75	2.62
B.E. (Y $P_D = 0\%$)	3.01	2.37	2.87	2.73

the form [9]

$$\lambda_n(E)\,\phi_{n,k_\alpha}(q,E) = \sum_{k_\beta} \int_0^\infty dq'\ K_{k_\alpha,k_\beta}^{JT}(q,q';E)\ \phi_{n;k_\beta}(q',E)\ , \tag{15}$$

where the kernel of the integral equations is given by

$$K_{k_\alpha,k_\beta}^{JT}(q,q';E) = Z_{k_\alpha,k_\beta}^{JT}(q,q';E)\ \tau_{k_\beta}[E - \epsilon_\beta(q')]\ q'^2\ , \tag{16}$$

with $Z_{k_\alpha,k_\beta}^{JT}$ being the Born amplitude for the exchange of particle γ and τ_{k_β} being the quasi-particle propagator for the pair $\gamma\alpha$ that was defined in Eq.(3). Here $\epsilon(q)$ is the energy of the spectator particle. In Eq.(15) the sum on the right hand side is over all three-body channels

for a given total angular momentum J and isospin T, and $\lambda_n(E)$ is the nth eigenvalue of the kernel at energy E. The position of the resonance pole is the energy E at which the largest eigenvalue of the kernel is one. Because resonances lie on the second energy sheet, we need to analytically continue Eqs.(15) and (16) onto that energy sheet. This is achieved by considering the transformation

$$q \to q\,e^{-i\theta} \qquad q' \to q'\,e^{-i\theta} \qquad \text{with} \qquad \theta > 0 \ . \tag{17}$$

This transformation exposes a section of the second energy plane between the ray defined by $|\arg \mathrm{E}| = 2\theta$ and the real axis. Thus, the part of the second Riemann sheet that is exposed is determined by how large we can make θ. The limitation on the rotation angle θ is imposed by the singularities of the kernel [13, 14]. Since both q and q' are rotated by the same angle, the Born amplitude $Z^{JT}_{k_\alpha, k_\beta}$ requires that $\theta < \frac{\pi}{2}$ [15], which gives us the region $\Im(E) < 0$ on the second Riemann sheet. The other source of singularity of the kernel is the quasi-particle propagator $\tau_{k_\beta}[E - \epsilon_\beta(q')]$. Because we have no nn or Λn bound states, the quasi-particle propagator τ_{k_β} has the two-body subsystem threshold branch point, and that generates the three-body threshold at $E = 0$. As a result, the only limitation on the contour rotation is that due to the Born amplitude. We therefore can perform any rotation with $\theta < \frac{\pi}{2}$.

Making use of the $^1\mathrm{S}_0$ nn potential defined in Eq.(14) and the $^1\mathrm{S}_0$ and $^3\mathrm{S}_1$ Λn potentials defined in Table I, we searched in the complex energy plane for the largest eigenvalue of the kernel having a value of one. We discovered such a 'resonance' pole at

$$E = -0.154 - 0.753\,i \text{ MeV} \quad \text{with an eigenvalue} \quad \lambda(E) = 1.0000 - 0.0001\,i \ . \tag{18}$$

However, because the $\Re(E) < 0$, this pole does not correspond to a resonance; it lies below the break-up threshold. Nevertheless, because the pole resides just below the threshold, we may ask the question: How easy is it to convert this pole into a true resonance or even into a bound state of the Λnn system? To explore this question we have scaled the strength of the Λn potential in both the $^1\mathrm{S}_0$ and $^3\mathrm{S}_1$ channels by a factor "s" and followed the path of this pole as it turns first into a resonance and then into a bound state. In Table III we give the energy of the pole and the corresponding eigenvalue of the kernel as we increase s in value. From this table we observe that a change of strength of as little as 7% produces a resonance above the three-body threshold, and a change of 35% will give us a bound Λnn system. For the resonance appearing just above threshold and corresponding to $s = 1.075$ with E

7

= 0.024 - 0.550i MeV, the singlet Λn scattering length becomes $a_s = -2.409$ fm and the effective range becomes $r_s = 3.462$ fm, which are closer to the values coming from the other three models given in Table II. For the threshold bound state corresponding to $s = 1.350$, the singlet scattering length and effective range would be -4.922 fm and 2.919 fm, which seem to be ruled out by Λp scattering data unless there exists a sizable charge symmetry breaking. Clearly ours is not a precision analysis, and the actual answer will depend on a more detailed model for the Λn and nn interactions.

TABLE III. We tabulate the energy E at which the largest eigenvalue of the kernel is $\lambda(E) = 1$ as we scale the Λn potential strength by the factor s.

s	E (MeV)	$\lambda(E)$
1.000	-0.154-0.753i	1.0000-0.0001i
1.025	-0.085-0.685i	1.0000-0.0001i
1.050	-0.026-0.618i	1.0000+0.0001i
1.075	0.024-0.550i	1.0000+0.0000i
1.100	0.063-0.483i	1.0000-0.0001i
1.125	0.095-0.418i	1.0000+0.0001i
1.150	0.116-0.353i	1.0000+0.0001i
1.175	0.130-0.291i	1.0000+0.0001i
1.200	0.135-0.232i	1.0000-0.0000i
1.225	0.132-0.177i	1.0000+0.0000i
1.250	0.121-0.126i	1.0000-0.0001i
1.275	0.102-0.081i	1.0000+0.0000i
1.300	0.077-0.043i	1.0000-0.0000i
1.325	0.043-0.014i	1.0000+0.0046i
1.350	0.000-0.000i	1.0000+0.0000i
1.375	-0.069-0.000i	Bound state
1.400	-0.158+0.000i	Bound state

As a measure of the uncertainty in our results, we considered the Λnn system with the NN and ΛN interactions in Tables IV and VI of Ref.[11] with a tensor force in the ΛN

potential. In this case the 'resonance' pole for $s = 1.0$ lies at

$$E = -0.107 - 0.622\,i \text{ MeV} \quad \text{with an eigenvalue} \quad \lambda(E) = 1.0000 - 0.0000\,i \,. \quad (19)$$

Then an increase in the strength scale s of 5% will produce a resonance at $E = 0.024 - 0.455\,i$ MeV, while an increase in strength of 25% will produce a threshold bound state in the Λnn system. In Fig. 1 we plot the trajectory of the 'resonance' pole as one increases the strength of the ΛN interaction. This illustrates how the sub threshold resonance turns into a bound state as one increases the strength of the potential, with unit scaling $s = 1.0$ corresponding to a sub threshold resonance at $E = -0.107 - 0.622\,i$ MeV and with increasing steps (red dots) of $\Delta s = 0.025$ to obtain a bound state with energy $E = -0.068$ MeV at $s = 1.250$ and $E = -0.195$ MeV for $s = 1.275$.
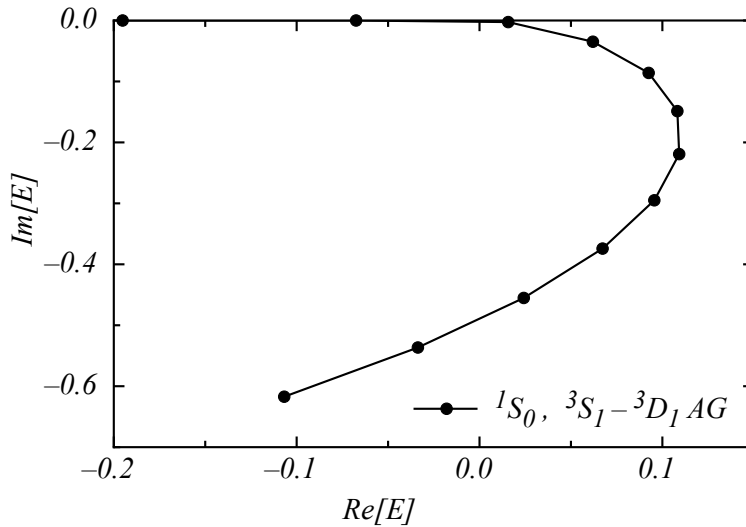

FIG. 1. Trajectory of the 'resonance' pole as one varies the strength of the ΛN interaction. In this case we have used the NN and ΛN interaction for Tables IV and VI of Ref.[11] with a tensor interaction for the ΛN potential.

One can plot a similar trajectory for different Λn interactions with the starting point corresponding for $s = 1.0$ depending on the scattering lengths and effective ranges of the Λn potential. In Fig. 2 we plot four different trajectories for the 'resonance' pole. In each case we use the same nn potential given in Eq. (14). For the Λn interaction we use the ${}^1S_0$ and ${}^3S_1$ (*i.e.*, no tensor force) that fit the effective range and scattering length from either the chiral model or meson exchange model. The Yamaguchi fits to these potentials

are given in Table II and are: Mod D for a fit to Nijmegen model D [5], Chiral for a fit to Chiral($\Lambda = 600$) [8], and NSC97f for a fit to Nijmegen NSC97f [6], and Jülich04 for the Jülich one boson exchange potential [7]. We first observe that all the curves are similar in that they trace the same shape as one varies the strength of the Λn interaction. However, the starting points for the four curves corresponding to $s = 1.0$ are all different, suggesting that a pole at a given energy will require a different scaling. This is illustrated in Table IV where we state the energy of the pole for $s = 1.0$ for the four different Λn potential curves plotted in Fig. 2. This demonstrates that the Jülich04 model gives a pole closest to being a resonance, while the Model D pole is farthest from being a resonance.
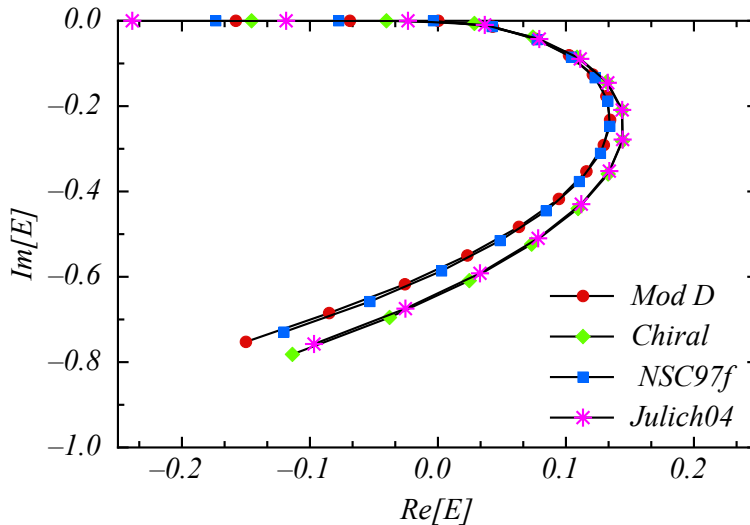

FIG. 2. (Color online) Trajectory of the 'resonance' pole as one varies the strength of the Λn interaction. In this case we use the same nn potential given in Eq. (14) for all four curves. The Λn potentials correspond to Yamaguchi fits as given in Table II with Mod D for Nijmegen model D, Chiral for Chiral($\Lambda = 600$), NSC97f for Nijmegen NSC97f, and Jülich04 for the Jülich one boson exchange potential.[a]

[a] In scaling the Λn potential we have insured that no two-body bound state is formed. For example, for Mod D the scaling of the potential by s=1.35 moved the two-body pole closest to the real axis from $k = -0.315\,i$ fm to $k = -0.164\,i$ fm.

The above trajectory for the pole in the Λnn amplitude, as one changes the strength s of the Λn potential, is interesting if we compare it with the equivalent situation in two-body scattering, where a bound-state pole on the first energy sheet moves onto the second energy

10

TABLE IV. The position of the pole of the Λnn amplitude for the four different Λn potentials considered in Fig. 2

Potential	Mod D	Chiral	NSC97f	Jülich04
Pole energy (MeV)	-0.154 - -0.753 i	-0.114-0.782 i	-0.120-0.730 i	-0.097-0.758 i

sheet, and often is referred to as an anti-bound state, as the strength of the interaction is reduced. On the other hand in the three-body system the bound-state pole turns into a resonance as the strength of the interaction is reduced. This difference is a result of the fact that in the two-body problem one has a square root branch point at $E = 0$, while for the three-body system we have a log branch point at $E = 0$. In the two-body system one has two Riemann energy sheets, while for the three-body system, with no bound state in the two-body subsystem, one has an infinity of Riemann energy sheets. As a result the bound state moves continuously onto the second sheet and becomes a resonance once the strength of the interaction is insufficient to support a three-body bound state. If the strength of the interaction is further weakened, the 'resonance' pole becomes a sub threshold resonance, moving to a region in the complex second Riemann sheet $Re(E) < 0$ where standard experiment cannot probe.

We should point out that this pole trajectory is similar to that of the three neutron case, but the scaling factor is quite different [16]. In particular, for the three neutron system, where the Pauli exclusion principle plays a significant role, one needs a substantial scaling factor to generate a resonance. In contrast, for the Λnn system, where there is no Pauli blocking, the required change in the strength of the Λn potential lies within the experimental uncertainty for this interaction. To illustrate this, we plot in Fig. 3 the changes in the Λn effective range parameters as one scales the potential. Here, we plot the variation of the singlet and triplet effective range parameters for Nijmegen Model D as function of s for $s = 1.0, \ldots, 1.275$ in intervals of $\Delta s = 0.025$. Also included in Fig. 3 are the effective range parameters for the potentials in Table II. It is clear from Fig. 3 that scaling the Λn potential to generate a resonance in the Λnn system does not require a change that is substantially different from the variation among the parameters for the different potentials. This suggests that one may be able to use this observation to place an experimental constraint on the Λn interaction.
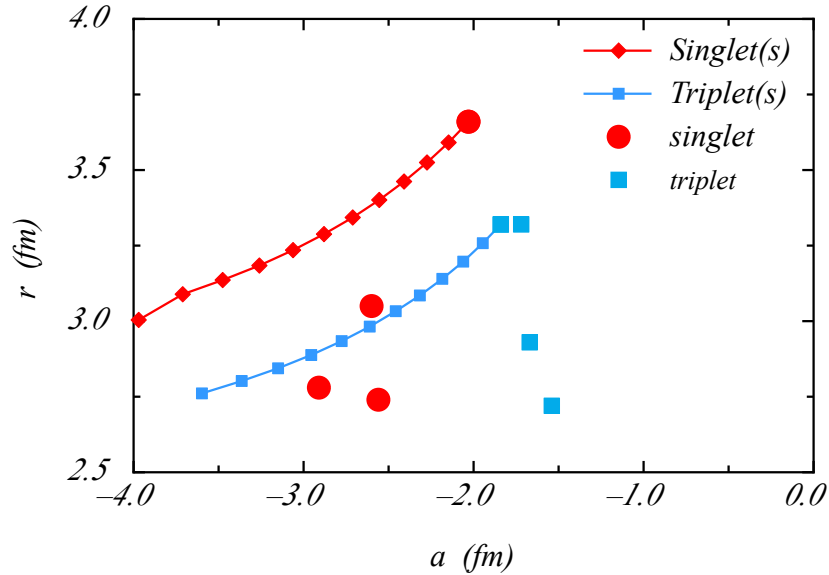
FIG. 3. (Color online) We plot the variation in the singlet (red) and triplet (blue) effective range parameter with variation in the the scaling s between $s = 1.0$ and $s = 1.275$ in intervals of $\Delta s = 0.025$. Also included are the effective range parameters of the four potentials considered in Table II.

V. CONCLUSIONS

In this analysis we have made use of Yamaguchi separable potentials that fit the effective range parameters of the NN interaction and the ΛN interaction as predicted by different models which reproduce the limited low energy scattering data for the Λp system. Use of the Yamaguchi potential allows us to explore the complex energy plane for the Λnn system seeking resonance poles. Although none of the potentials examined predict a resonance pole, we show that a scaling of the Λn interaction by as little as $\sim 5\%$ could produce a resonance in the Λnn system, and a scaling of $\sim 25\%$ would produce a Λnn bound state. This suggests that one may use photo (electro) production of the Λnn system as a tool to examine the strength of the Λn interaction. In particular, K^+ electro production from tritium at JLab would be a means to explore for a possible Λnn resonance in the final state; modeling the position and shape of such a resonance would provide constraints on the properties of the un-measured Λn interaction. A more detailed analysis of the Λnn system based on more realistic interactions including tensor forces, coupling of ΛN to ΣN, and a three-body force might suggest how sensitive the energy of the resonance is to the details of the Λn interaction.

12

Following completion of this work it came to our attention that Belyaev *et al.* [17] had earlier explored the $nn\Lambda$ bound-state and resonance problem. They worked in coordinate space using hyperspherical harmonics at lowest order and searched for the zero in the Jost function. They found no bound state but did see a broad resonance (width greater than 2 MeV); to obtain a bound state they required a scaling factor of 1.5, about twice that which we found necessary to generate a threshold bound state.

VI. ACKNOWLEDGEMENT

[1] C. Rappold, *et al.*, "Search for evidence of $^{3}_{\Lambda}n$ by observing $d + \pi^-$ and $t + \pi^-$ final states in the reaction of ^{6}Li+^{12}C at $2A$ GeV", Phys. Rev. C **88**, 041001(R) (2013).

[2] H. Garcilazo, and A.Valcarce, "Nonexistance of a Λnn bound state", Phys. Rev. C**89**, 057001 (2014).

[3] E. Hiyama, S. Ohnishi, B. F. Gibson, and Th. A. Rijken, "Three-body structure of the $nn\Lambda$ system with $\Lambda N - \Sigma N$ coupling", Phys. Rev. C **89**, 061302(R) (2014).

[4] A. Gal, and H. Garcilazo, "Is there a bound $^{3}_{\Lambda}$n?", Phys. Lett. **B736**, 93 (2014).

[5] M. M. Nagels, T. A. Rijken, and J. J. de Swart, "Baryon-baryon scattering in a one-boson-exchange-potential approach, II. Hypron-nucleon scattering", Phys, Rev. D **15**, 2547 (1977).

[6] T. A. Rijken, V. G. J. Stoks, Y. Yamamoto, "Soft-core hypron-nucleon potentials", Phys. Rev. C **59**, 21 (1999).

[7] J. Haidenbauer and Ulf-G. Meißner, "Jülich hypron-nucleon model revisited", Phys. Rev. C **72**, 044005 (2005).

[8] J. Haidenbauer, *et al.*, "Hypron-nucleon interaction at next-to-leading order in chiral effective field theory", Nucl. Phys. A **915**, 24 (2013).

[9] I. R. Afnan and B. F. Gibson, "Resonances in Λd scattering and the Σ hypertriton", Phys. Rev. C **47**, 1000 (1993).

[10] Y. Yamaguchi, "Two-Nucleon Problem When the Potential Is Nonlocal but Separable. I", Phys. Rev. **95**, 1628 (1954).

[11] I. R. Afnan and B. F. Gibson, "Hypertriton: $\Lambda \leftrightarrow \Sigma$ conversion and tensor force", Phys. Rev. C **41**, 2787 (1990).

[12] Q. Chen, *et al.*, "Measurement of the neutron-neutron scattering length using the $\pi^- d$ capture reaction", Phys. Rev. C **77**, 054002 (2008).

[13] B. C. Pearce and I. R. Afnan, "Resonance poles in three-body systems", Phys. Rev. C **30**, 2022 (1984).

[14] I. R. Afnan, "Resonances in Few-Body Systems", Aust. J. Phys. **44**, 201 (1991).

[15] A. T. Stelbovics, "On the application of contour rotation to three-body amplitudes", Nucl. Phys. **A288**, 461 (1977).

[16] R. Lazauskas and J. Carbonell, "Three-neutron resonance trajectory for realistic interaction models", Phys. Rev. C **71**, 044004 (2005). See also references within.

[17] V. B. Bleyaev, S. A. Rakityansky, and W. Sandhas, "Three-body resonances Λnn and $\Lambda\Lambda n$" Nucl. Phys. **A 803**, 210 (2008).